Computer Assisted Mechanics and Engineering Sciences, 10: 33–43, 2003.

Limitation of the single-domain numerical approach: Comparisons of analytical and numerical solutions for a forced convection heat transfer problem in a composite duct

Andrey V. Kuznetsov
Department of Mechanical and Aerospace Engineering, North Carolina State University
Campus Box 7910, Raleigh, NC 27695-7910, U.S.A.

(Received November 16, 2000)

The aim of this paper is to establish the bounds of applicability of the single-domain numerical approach for computations of convection in composite porous/fluid domains. The large number of papers that have utilized this numerical approach motivates this research. The popularity of this approach is due to the simplicity of its numerical formulation. Since the utilization of the single-domain numerical approach does not require the explicit imposing of any boundary conditions at the porous/fluid interface, the aim of the this research is to investigate whether this method always produces accurate numerical solutions.

NOMENCLATURE

A – parameter defined by Eq. (24)
B – parameter defined by Eq. (20)
c_f – specific heat at constant pressure, J/(kg K)
c_F – Forchheimer coefficient
D – parameter defined by Eq. (21)
Da – Darcy number, K/H^2
F – scaled Forchheimer coefficient, $(\rho_f c_F H^4 G)/(K^{1/2}\mu_f^2)$
G – applied pressure gradient, $-\mathrm{d}\tilde{p}/\mathrm{d}\tilde{x}$, Pa/m
H – half parallel plate separation distance, m
k_f – thermal conductivity of the fluid, W/(m K)
k_{eff} – effective thermal conductivity of the porous medium, W/(m K)
k_s – thermal conductivity of the solid phase in the porous region, W/(m K)
K – permeability of the porous medium, m^2
l – coordinate of the center of the porous layer, m
L – dimensionless coordinate of the center of the porous layer, l/H
Nu – Nusselt number, $2Hq''/\left[k_f(\tilde{T}_W - \tilde{T}_m)\right]$
$\tilde{p}$ – intrinsic average pressure, Pa
P – parameter defined by Eq. (29)
q'' – wall heat flux, $\mathrm{W/m^2}$
Q – parameter defined by Eq. (27)
R – thermal conductivity ratio, k_{eff}/k_f
s – half thickness of the clear fluid region, m
S – dimensionless half thickness of the clear fluid, s/H
T – dimensionless temperature, $(\tilde{T} - \tilde{T}_W)/(\tilde{T}_m - \tilde{T}_W)$

T_i – dimensionless temperature at the clear fluid/porous medium interface
$\tilde{T}$ – intrinsic average temperature, K
$\tilde{T}_m$ – mean temperature, K
$\tilde{T}_W$ – wall temperature, K
u – dimensionless velocity, $(\tilde{u}_f \mu_f)/(GH^2)$
u_1 – parameter defined by Eq. (19)
u_∞ – dimensionless velocity between the momentum boundary layers, in the center of the porous region
$\tilde{u}_f$ – filtration (seepage) velocity, m/s
u_i – dimensionless velocity at the clear fluid/porous medium interface
$\tilde{U}$ – mean velocity, m/s
U – dimensionless mean velocity
$\tilde{x}$ – streamwise coordinate, m
$\tilde{y}$ – transverse coordinate, m
y – dimensionless transverse coordinate, $\tilde{y}/H$
z_1 – function of the coordinate y defined by Eq. (23)
z_2 – function of the coordinate y defined by Eq. (18)

Greek letters

β – adjustable coefficient in the representation for the excess stress at the interface
γ – constant, $(\mu_{\text{eff}}/\mu_f)^{1/2}$
ε – porosity of the porous region
μ_f – fluid viscosity, $\text{kg m}^{-1}\,\text{s}^{-1}$
μ_{eff} – effective viscosity in the Brinkman term for the porous region, $\text{kg m}^{-1}\,\text{s}^{-1}$
ρ_f – density of the fluid, kg m^{-3}
ϕ – ratio of the dimensionless temperature to the Nusselt number, T/Nu

1. Introduction

The main purpose of this paper is to investigate the bounds of applicability of the single-domain numerical approach. This numerical approach has become increasingly popular in recent years for handling convection problems in composite domains that consist of both porous and clear fluid regions. An example of such a problem is the investigation of natural convection during the solidification of a binary alloy in an enclosure. During the solidification of a binary alloy, there are generally three regions in the computational domain: one occupied by the solid phase, another by the mushy (two-phase) zone, and a third by liquid alloy. A direct numerical solution of this problem requires the numerical modeling of boundary conditions at two interfaces, between the solid region and the mushy zone and between the liquid region and the mushy zone. Because these interfaces move during the solidification process it is necessary to track their positions at all times.

The single-domain approach suggests a much simpler alternative to this complicated numerical procedure. In the single-domain approach, governing equations are written in such form that they reduce to the correct limits in all three zones of the computational domain. Utilizing differential governing equations whose coefficients make a jump when crossing the interface accomplishes this. The coefficient of the Darcy term, for example, is unity in the mushy zone whereas it is zero in the liquid zone. Since these governing equations are valid in the entire computational domain, no boundary conditions at the liquid/mushy and solid/mushy interfaces are required to obtain their solution. Only the boundary conditions at the external boundaries of the domain are needed. Examples of the successful application of the single-domain approach to solidification problems

include Beckermann and Viskanta [1], Bennon and Incropera [3], Schneider and Beckermann [19], Yoo and Viskanta [22], Voller and Prakash [21], along with many others.

Another example of a problem for which the solution of the single-domain numerical approach has been utilized is the computation of convection heat transfer in a composite domain that is partly occupied by a clear fluid and partly by fluid-saturated porous medium. This problem is relevant to many industrial applications, such as microelectronic cooling. Examples of the successful application of the single-domain approach to the investigation of convection in composite domains include, but are not limited to, Vafai and Kim [20], Huang and Vafai [7], Kim and Choi [9], and Hadim [6].

The simplification of the numerical algorithm attained due to the utilization of the single-domain approach is very impressive. Using this technique, there is no need to solve a numerical problem in a number of computational sub-domains, each of which has a moving boundary. Instead, it is only necessary to solve the problem in one domain with simple fixed boundaries and external boundary conditions that are usually simple as well.

The main limitation of the single-domain approach is closely related to its main advantage, the impossibility of explicit imposing of any boundary conditions at the interfaces inside the computational domain. The utilization of the single-domain approach for porous/fluid composite domains results in numerical solutions that automatically satisfy the continuity of velocities, shear stresses, temperatures, and heat fluxes across the porous/fluid interface [20]. As it was shown in Nield [14], continuity of filtration velocity across the interface is a correct condition. Indeed, the interface of the porous medium contains both pores and solid particles. In the pores, the fluid velocity in the porous medium matches with the fluid velocity outside the medium. Over the solid part of the interface, the velocity is zero both in the solid and in the adjacent clear fluid because of the no-slip condition. However, the condition of continuity of shear stresses across the interface is not necessarily a correct condition. Over the pore section of the interface, the velocity shear is continuous. Over the solid section this is not necessarily the case. Velocity shear is identically zero in the solid, but in the adjacent clear fluid it may take on a non-zero value.

A formal mathematical investigation of boundary conditions at the porous/fluid interface was carried out by Ochoa-Tapia and Whitaker [16, 17]. In these papers, by means of a complex volume averaging analysis of the momentum equations in the interface region, it was shown that though matching the Brinkman–Darcy and Stokes equation retains continuity of velocity, it may produce a jump in the shear stress. This explains the major limitation of the single domain approach for composite porous/fluid systems. Numerical solutions obtained by the single-domain approach always satisfy continuity of the shear stress condition, they cannot account for a possible jump in the shear stress at the porous/fluid interface. This paper investigates whether the failure to account for the possible jump in the shear stress at the interface may result in considerable deviation of the single-domain numerical solutions from exact solutions for flow velocity, temperature, and Nusselt number.

2. Statement of the problem

Figure 1 displays a schematic diagram of the problem (only half of the channel is displayed because of symmetry). A parallel-plate channel is composed of two porous layers that are attached to the walls and a clear fluid region in the center. The walls of the channel are subject to a uniform heat flux. The set of governing equations for this problem is as follows,

$$-\frac{\mathrm{d}\tilde{p}}{\mathrm{d}\tilde{x}} + \frac{\mathrm{d}}{\mathrm{d}\tilde{y}}\left(\mu_f \frac{\mathrm{d}\tilde{u}_f}{\mathrm{d}\tilde{y}}\right) = 0, \qquad 0 \le \tilde{y} \le s, \tag{1}$$

$$-\frac{\mathrm{d}\tilde{p}}{\mathrm{d}\tilde{x}} + \frac{\mathrm{d}}{\mathrm{d}\tilde{y}}\left(\mu_{\mathrm{eff}} \frac{\mathrm{d}\tilde{u}_f}{\mathrm{d}\tilde{y}}\right) - \frac{\mu_f}{K}\tilde{u}_f - \frac{\rho_f c_F}{K^{1/2}}\tilde{u}_f^2 = 0, \qquad s \le \tilde{y} \le H, \tag{2}$$

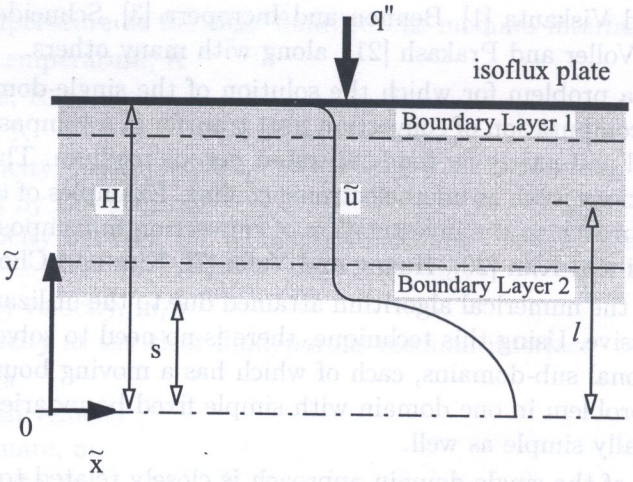

Fig. 1. Schematic diagram of the problem

$$\rho_f c_f \tilde{u}_f \frac{\partial \tilde{T}}{\partial \tilde{x}} = \frac{\mathrm{d}}{\mathrm{d}\tilde{y}} \left(k_f \frac{\mathrm{d}^2 \tilde{T}}{\mathrm{d}\tilde{y}^2} \right), \qquad 0 \le \tilde{y} \le s, \tag{3}$$

$$\rho_f c_f \tilde{u}_f \frac{\partial \tilde{T}}{\partial \tilde{x}} = \frac{\mathrm{d}}{\mathrm{d}\tilde{y}} \left(k_{\mathrm{eff}} \frac{\mathrm{d}\tilde{T}}{\mathrm{d}\tilde{y}} \right), \qquad s \le \tilde{y} \le H, \tag{4}$$

where c_f is the specific heat of the fluid, c_F is the Forchheimer coefficient, H is half the distance between the plates of the channel, k_f is the thermal conductivity of the fluid, k_{eff} is the thermal conductivity of the porous medium, K is the permeability of the porous medium, $\tilde{p}$ is the pressure, s is the thickness of the clear fluid region, $\tilde{T}$ is the temperature, $\tilde{u}_f$ is the filtration (seepage) velocity, $\tilde{x}$ is the streamwise coordinate, $\tilde{y}$ is the transverse coordinate, μ_f is the fluid viscosity, μ_{eff} is the effective viscosity in the Brinkman term for the porous region, and ρ_f is the density of the fluid. Equation (1) is the momentum equation for the clear fluid region while Eq. (2) is the momentum equation for the porous region (the Brinkman–Forchheimer–extended Darcy equation). Equations (3) and (4) are the energy equations for the clear fluid and porous regions, respectively. Following [4, 8, 13, 15], longitudinal heat conduction is neglected in Eqs. (3) and (4). This assumption is acceptable for large Péclet numbers.

In Eq. (2), the fluid viscosity, μ_f, and the effective viscosity in the Brinkman term, μ_{eff}, are distinct. Most works that have used the Brinkman model assumed that $\mu_{\mathrm{eff}} = \mu_f$. However, recent direct numerical simulations (such as Martys et al. [12]) as well as experimental investigations (Givler and Altobelli [5]) have demonstrated that there are situations when it is important to distinguish between these two coefficients. For example, in Givler and Altobelli [5], a water flow through a tube filled with open-cell rigid foam of high porosity was investigated. It was obtained that, for this flow, $\mu_{\mathrm{eff}} = \left(7.5^{+3.4}_{-2.4}\right) \mu_f$.

At the porous/fluid interface the boundary conditions suggested by Ochoa-Tapia and Whitaker [16, 17] are utilized,

$$\tilde{u}_f|_{\tilde{y}=s-0} = \tilde{u}_f|_{\tilde{y}=s+0}, \qquad \mu_{\mathrm{eff}} \left.\frac{\mathrm{d}\tilde{u}_f}{\mathrm{d}\tilde{y}}\right|_{\tilde{y}=s+0} - \mu_f \left.\frac{\mathrm{d}\tilde{u}_f}{\mathrm{d}\tilde{y}}\right|_{\tilde{y}=s-0} = \beta \frac{\mu_f}{K^{1/2}} \tilde{u}_f|_{\tilde{y}=s}, \qquad \text{at} \quad \tilde{y} = s, \tag{5}$$

$$\tilde{T}\Big|_{\tilde{y}=s-0} = \tilde{T}\Big|_{\tilde{y}=s+0}, \qquad k_{\mathrm{eff}} \left.\frac{\partial \tilde{T}}{\partial \tilde{y}}\right|_{\tilde{y}=s+0} = k_f \left.\frac{\partial \tilde{T}}{\partial \tilde{y}}\right|_{\tilde{y}=s-0}, \qquad \text{at} \quad \tilde{y} = s, \tag{6}$$

where β is the adjustable coefficient in the stress jump boundary condition.

The boundary conditions in the center of the channel and at the peripheral wall are given by the following,

$$\frac{\partial \tilde{u}_f}{\partial \tilde{y}} = 0, \qquad \frac{\partial \tilde{T}}{\partial \tilde{y}} = 0, \qquad \text{at} \quad \tilde{y} = 0, \tag{7}$$

$$\tilde{u}_f = 0, \qquad k_{\text{eff}} \frac{\partial \tilde{T}}{\partial \tilde{y}} = q'', \qquad \text{at} \quad \tilde{y} = H, \tag{8}$$

respectively, where q'' is the wall heat flux.

3. ANALYTICAL SOLUTION

The appropriate dimensionless velocity, temperature, and Nusselt number for this problem can be defined as

$$u = \frac{\tilde{u}_f \mu_f}{GH^2}, \tag{9}$$

$$T = \frac{\tilde{T} - \tilde{T}_W}{\tilde{T}_m - \tilde{T}_W}, \tag{10}$$

$$Nu = \frac{2Hq''}{k_f(\tilde{T}_W - \tilde{T}_m)}, \tag{11}$$

where G is the applied pressure gradient ($= -\mathrm{d}\tilde{p}/\mathrm{d}\tilde{x}$), $\tilde{T}_W$ is the wall temperature, and $\tilde{T}_m$ is the mean flow temperature, and $\tilde{U}$ is the mean flow velocity. The mean flow temperature is defined by the following expression,

$$\tilde{T}_m = \frac{1}{H\tilde{U}} \int_0^H \tilde{u}_f \tilde{T} \, \mathrm{d}\tilde{y}. \tag{12}$$

The mean flow velocity is defined as

$$\tilde{U}_m = \frac{1}{H} \int_0^H \tilde{u}_f \, \mathrm{d}\tilde{y}. \tag{13}$$

Kuznetsov [10] obtained a solution to this problem utilizing the boundary layer approach. The main assumption utilized in that paper was that the momentum boundary layers in the porous region (one of which is attached to the solid wall while the other is attached to the clear fluid/porous medium interface) do not overlap in the center of the porous layer (Fig. 1). Utilizing this approach, the velocity in the channel was obtained as follows.

The velocity distribution in the clear fluid region ($0 \leq y \leq S$) was obtained as

$$u = u_i + \frac{S^2 - y^2}{2} \tag{14}$$

where y is the dimensionless transverse coordinate ($= \tilde{y}/H$) and u_i is the dimensionless velocity at the clear fluid/porous medium interface, which can be computed from the following transcendental equation,

$$-\gamma(u_i - u_\infty)\left[\frac{2}{3}F(u_i + u_1)\right]^{1/2} + S = \beta Da^{-1/2} u_i \tag{15}$$

where Da is the Darcy number (defined by K/H^2), F is the scaled Forchheimer coefficient $(\rho_f c_F H^4 G)/(K^{1/2}\mu_f^2)$, and u_∞ is the dimensionless velocity between the momentum boundary layers at the center of the porous region. This velocity is given by

$$u_\infty = \frac{-1 + [1 + 4Da^2 F]^{1/2}}{2Da\,F}. \tag{16}$$

The velocity distribution in the boundary layer 2 region ($S \le y \le L$) was obtained as

$$u = (u_\infty + u_1)\left[\frac{1 - z_2}{1 + z_2}\right]^2 - u_1 \tag{17}$$

where

$$z_2 = B\,\exp\{-D(y - S)\}, \tag{18}$$

$$u_1 = 2u_\infty + \frac{3}{2DaF}, \tag{19}$$

$$B = \frac{1 - \left[\frac{u_i + u_1}{u_\infty + u_1}\right]^{1/2}}{1 + \left[\frac{u_i + u_1}{u_\infty + u_1}\right]^{1/2}}, \tag{20}$$

$$D = \frac{1}{\gamma}\left[\frac{2F(u_\infty + u_1)}{3}\right]^{1/2}. \tag{21}$$

Finally, the velocity distribution in the boundary layer 1 ($L \le y \le 1$) region was obtained as

$$u = (u_\infty + u_1)\left[\frac{z_1 - 1}{z_1 + 1}\right]^2 - u_1 \tag{22}$$

where

$$z_1 = A\,\exp\{D(1 - y)\} \tag{23}$$

and

$$A = \frac{1 + \left[\frac{u_1}{u_\infty + u_1}\right]^{1/2}}{1 - \left[\frac{u_1}{u_\infty + u_1}\right]^{1/2}}. \tag{24}$$

The dimensionless temperature in the clear fluid region ($0 \le y \le S$) was obtained as

$$T = T_i + \frac{Nu}{U}\left[\left(\frac{u_i}{2} + \frac{S^2}{4}\right)(S^2 - y^2) - \frac{1}{24}(S^4 - y^4)\right]. \tag{25}$$

The dimensionless temperature in the boundary layer 2 region was obtained as

$$T = T_i - \frac{1}{R}\frac{Nu}{U}\left\{Q(y - S) + \frac{u_\infty}{2}(y - S)^2 - \frac{6\gamma^2}{F}\ln\frac{1 + B\exp\{-D(y - S)\}}{1 + B}\right\} \tag{26}$$

where

$$Q = u_i S + \frac{S^3}{3} - \frac{2\sqrt{6}\,\gamma(u_\infty + u_1)^{1/2} B}{F^{1/2}(1 + B)}. \tag{27}$$

The dimensionless temperature in the boundary layer 1 region was obtained as

$$T = Nu\frac{1}{RU}\left\{(1-y)P + \frac{u_\infty}{2}(y+1-2L)(1-y) + \frac{6\gamma^2}{F}\ln\frac{1+A\exp\{D(1-y)\}}{1+A}\right\} \tag{28}$$

where

$$P = Q + u_\infty(L-S) - \frac{2\sqrt{6}\,\gamma(u_\infty+u_1)^{1/2}}{F^{1/2}\,(1+B\,\exp\{-D(L-S)\})} + \frac{2\sqrt{6}\,\gamma(u_\infty+u_1)^{1/2}}{F^{1/2}\,(1+A\,\exp\{D(1-L)\})}. \tag{29}$$

The dimensionless temperature at the clear fluid/porous medium interface, T_i, was found by matching the temperature distributions given by Eqs. (26) and (28) at $y = L$.

Finally, the Nusselt number was found from the compatibility condition (Bejan [2]),

$$Nu = \frac{U}{\int_0^1 u\phi\,\mathrm{d}y} \tag{30}$$

where

$$U = \frac{\tilde{U}\mu_f}{GH^2} \tag{31}$$

and

$$\phi = T/Nu. \tag{32}$$

The dependence $\phi = \phi(y)$, which is necessary to resolve Eq. (30), follows from Eqs. (25), (26), and (28).

4. NUMERICAL SOLUTION USING THE SINGLE-DOMAIN APPROACH

For the purposes of the single-domain numerical solution, momentum equations (1) and (2) can be combined into one equation that is valid throughout the computational domain ($0 \le y \le 1$), in both the porous and clear fluid regions. Utilizing dimensionless variables, this equation can be presented as

$$1 + \frac{\mathrm{d}}{\mathrm{d}y}\left(\sigma_1\frac{\mathrm{d}u}{\mathrm{d}y}\right) - \sigma_2\frac{1}{Da}u - \sigma_3 F u^2 = 0 \tag{33}$$

where for $0 \le y \le S$

$$\sigma_1 = 1, \qquad \sigma_2 = \sigma_3 = 0, \tag{34}$$

and for $S \le y \le 1$

$$\sigma_1 = \gamma^2, \qquad \sigma_2 = \sigma_3 = 1. \tag{35}$$

Energy equations (3) and (4) can also be combined into one equation that is valid throughout the computational domain ($0 \le y \le 1$). In dimensionless variables this equation can be presented as

$$\frac{\mathrm{d}}{\mathrm{d}y}\left(\sigma_4\frac{\mathrm{d}\phi}{\mathrm{d}y}\right) = -\frac{1}{2}\frac{u}{U} \tag{36}$$

where for $0 \le y \le S$

$$\sigma_4 = 1 \tag{37}$$

and for $S \leq y \leq 1$

$$\sigma_4 = R. \tag{38}$$

Equations (33) and (36) must be solved subject to the following boundary conditions,

$$\frac{\partial u}{\partial y} = 0 \quad \text{and} \quad \frac{\partial T}{\partial y} = 0 \qquad \text{at} \quad y = 0, \tag{39}$$

$$u = 0 \quad \text{and} \quad T = 0 \qquad \text{at} \quad y = 1. \tag{40}$$

A harmonic-mean formulation (Patankar [18]) is adopted for the interface diffusion coefficients between two control volumes. This approach is capable of handling abrupt changes in these coefficients at the fluid/porous interface. Once the velocity and temperature profiles are computed, the Nusselt number is computed utilizing compatibility condition (30).

5. Results and Discussion

Figure 2 presents the velocity distributions computed utilizing numerical and analytical solutions for different values of β. According to Eq. (5), the parameter β characterizes the jump in the shear stress at the porous/fluid interface, and $\beta = 0$ corresponds to the situation when the shear stress is continuous through the interface. Figure 2 shows that numerical and analytical solutions coincide only when $\beta = 0$. The single-domain numerical solution cannot account for a discontinuity of the shear stress at the interface because the parameter β is not present in the numerical formulation at all. Therefore, if this discontinuity is required by the physics of the problem, an alternative numerical method should be used, which would allow for the specification of boundary conditions at the interface, directly.

This conclusion is in agreement with the findings of [11], where the validity of the single-domain numerical approach for the solution of the fluid flow problem in composite ducts has been investigated. Ref. [11], however, did not address the heat transfer situation, and the main purpose of this investigation is to analyze the accuracy of the single-domain approach in resolution of both the fluid flow and heat transfer in a composite channel.

Figure 3 depicts the temperature distributions in the channel computed for different values of the parameters β. This figure shows that, like for the filtration velocity distributions, the analytical and numerical temperature distributions coincide only for the case of $\beta = 0$. This is because the velocity distribution influences the temperature distribution through the convection term in the energy

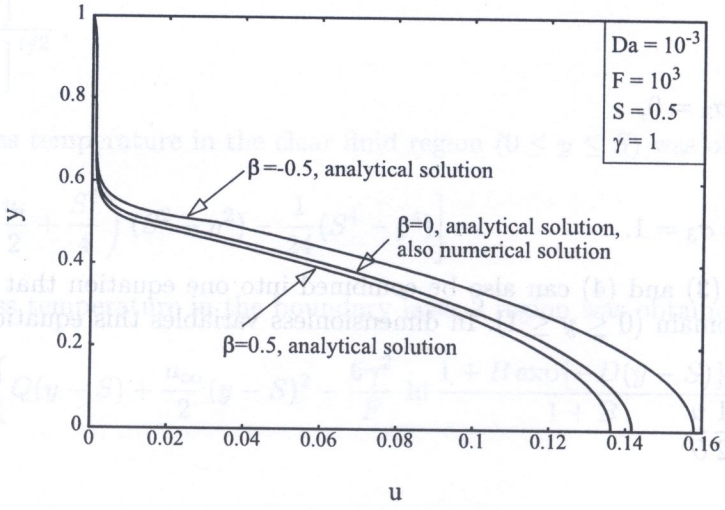

Fig. 2. Effect of parameter β on the numerically and analytically obtained velocity distributions in the channel

equation, therefore if the numerical velocity distribution is incorrect, the temperature distribution is also incorrect.

Figure 4 depicts the dependence of the Nusselt number in the channel on the Darcy number for different values of parameters β. As expected, the single-domain numerical solution is correct only when $\beta = 0$. A small but visible difference between the numerical and analytical solutions for $\beta = 0$ in Fig. 4 for large Darcy numbers exists because the analytical solution obtained in [10] is based on the boundary layer approximation that is valid only as long as the momentum boundary layers do not overlap in the center of the porous region. The thickness of the boundary layers increases with an increase in the Darcy number; and for large Darcy numbers the analytical solution gives incorrect results. This is why the analytical solution deviates from the numerical solution for $\beta = 0$ in Fig. 4 when the Darcy number approaches 10^{-2}.

Figure 5 displays the dependence of the Nusselt number on the dimensionless thickness of the clear fluid region ($S = 0$ corresponds to the channel completely occupied by the porous medium and $S = 1$ corresponds to the channel completely occupied by the clear fluid) for different values of parameters β. As expected, the single-domain numerical solution coincides with the analytical

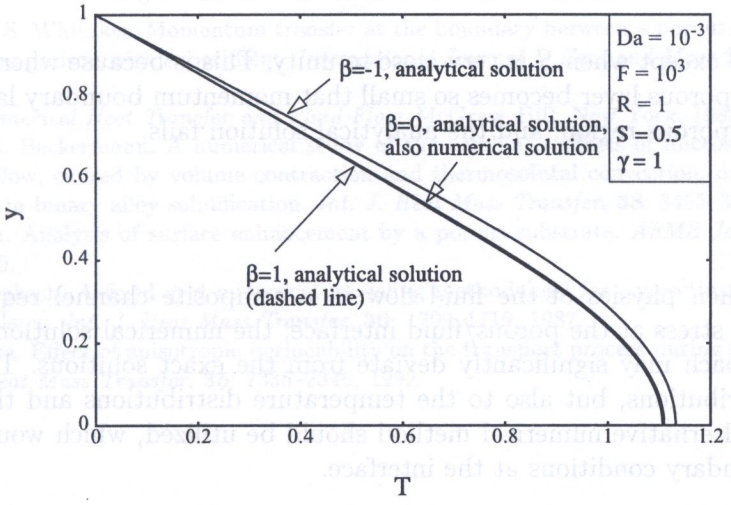

Fig. 3. Effect of parameter β on the numerically and analytically obtained temperature distributions in the channel

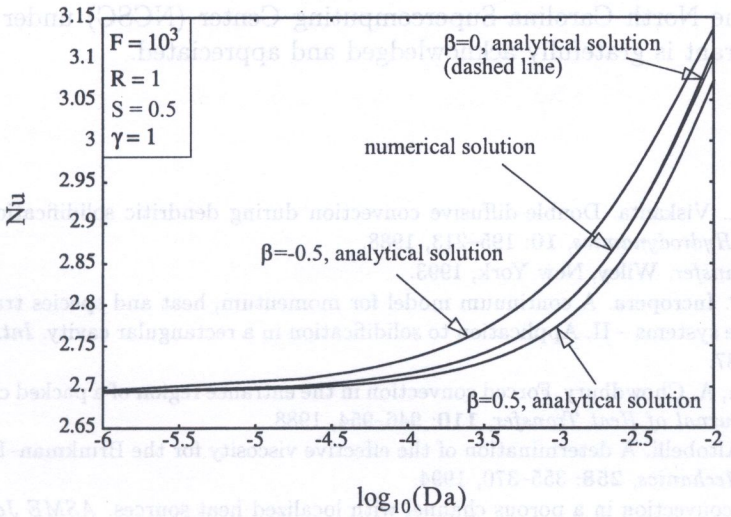

Fig. 4. Effect of parameter β on the numerically and analytically obtained dependencies of the Nusselt number on the Darcy number

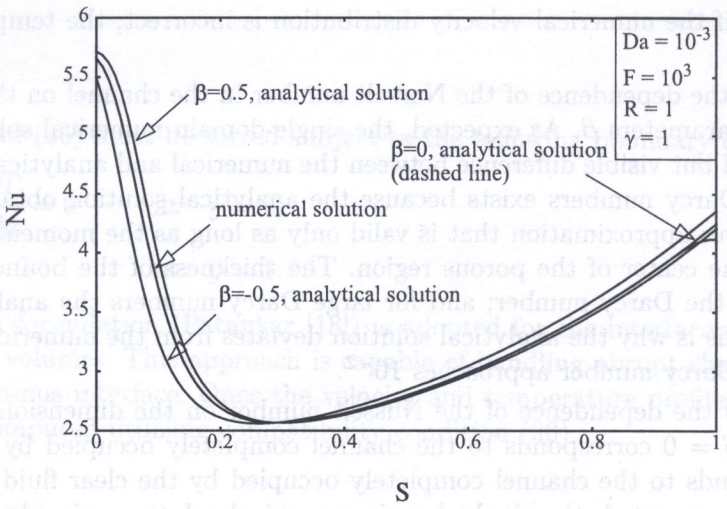

Fig. 5. Effect of parameter β on the numerically and analytically obtained dependencies of the Nusselt number on the thickness of the clear fluid region

solution when $\beta = 0$ except when S is very close to unity. This is because when S approaches unity the thickness of the porous layer becomes so small that momentum boundary layers start to overlap in the center of the porous region, and the analytical solution fails.

6. Conclusions

It is shown that when physics of the fluid flow in a composite channel requires accounting for a jump in the shear stress at the porous/fluid interface, the numerical solutions obtained from the single-domain approach may significantly deviate from the exact solutions. This applies not only to the velocity distributions, but also to the temperature distributions and the Nusselt numbers. In such a case, an alternative numerical method should be utilized, which would allow for a direct specification of boundary conditions at the interface.

Acknowledgement

The assistance of the North Carolina Supercomputing Center (NCSC) under an Advanced Computing Resources Grant is gratefully acknowledged and appreciated.

References

[1] C. Beckermann, R. Viskanta. Double-diffusive convection during dendritic solidification of a binary mixture. *Physico-Chemical Hydrodynamics*, **10**: 195–213, 1988.

[2] A. Bejan. *Heat Transfer*. Wiley, New York, 1993.

[3] W.D. Bennon, F.P. Incropera. A continuum model for momentum, heat and species transport in binary solid–liquid phase change systems – II. Application to solidification in a rectangular cavity. *Int. J. Heat Mass Transfer*, **30**: 2171–2187, 1987.

[4] P. Cheng, C.T. Hsu, A. Chowdhury. Forced convection in the entrance region of a packed channel with asymmetric heating. *ASME Journal of Heat Transfer*, **110**: 946–954, 1988.

[5] R.C. Givler, S.A. Altobelli. A determination of the effective viscosity for the Brinkman–Forchheimer flow model. *Journal of Fluid Mechanics*, **258**: 355–370, 1994.

[6] A. Hadim. Forced convection in a porous channel with localized heat sources. *ASME Journal of Heat Transfer*, **116**: 465–472, 1994.

[7] P.C. Huang, K. Vafai. Flow and heat transfer control over an external surface using a porous block arrangement. *International Journal of Heat and Mass Transfer*, **36**: 4019–4032.

[8] M. Kaviany. Laminar flow through a porous channel bounded by isothermal parallel plates. *International Journal of Heat and Mass Transfer*, **28**: 851–858, 1985.

[9] S.J. Kim, C.Y. Choi. Convective heat transfer in porous and overlying fluid layers heated from below. *International Journal of Heat and Mass Transfer*, **39**: 319–329, 1993.

[10] A.V. Kuznetsov. Analytical study of fluid flow and heat transfer during forced convection in a composite channel partly filled with a Brinkman–Forchheimer porous medium. *Flow, Turbulence and Combustion*, **60**: 173–192, 1998.

[11] A.V. Kuznetsov, M. Xiong. On the limitations of the single-domain approach for computation of convection in composite channels – Comparisons with exact solutions. *Hybrid Methods in Engineering*, **1**: 249–264, 1999.

[12] N. Martys, D.P. Bentz, E.J. Garboczi. Computer simulation study of the effective viscosity in Brinkman's equation. *Phys. Fluids*, **6**: 1434–1439, 1994.

[13] A. Nakayama, H. Koyama, F. Kuwahara. An analysis on forced convection in a channel filled with a Brinkman–Darcy porous medium: Exact and approximate solutions. *Wärme- und Stoffübertragung*, **23**: 291–295, 1988.

[14] D.A. Nield. The limitations of the Brinkman–Forchheimer equation in modeling flow in a saturated porous medium and at an interface. *International Journal of Heat and Fluid Flow*, **12**: 269–272, 1991.

[15] D.A. Nield, S.L.M. Junqueira, J.L. Lage. Forced convection in a fluid saturated porous medium channel with isothermal or isoflux boundaries. *Journal of Fluid Mechanics*, **322**: 201–214, 1996.

[16] J.A. Ochoa-Tapia, S. Whitaker. Momentum transfer at the boundary between a porous medium and a homogeneous fluid – I. Theoretical development. *International Journal of Heat and Mass Transfer*, **38**: 2635–2646, 1995.

[17] J.A. Ochoa-Tapia, S. Whitaker. Momentum transfer at the boundary between a porous medium and a homogeneous fluid – II. Comparison with experiment. *International Journal of Heat and Mass Transfer*, **38**: 2647–2655, 1995.

[18] S.V. Patankar. *Numerical Heat Transfer and Fluid Flow*. McGraw–Hill, New York, 1980.

[19] M.C. Schneider, C. Beckermann. A numerical study of the combined effects of microsegregation, mushy zone permeability and flow, caused by volume contraction and thermosolutal convection, on macrosegregation and eutectic formation in binary alloy solidification. *Int. J. Heat Mass Transfer*, **38**: 3455–3473, 1995.

[20] K. Vafai, S.J. Kim. Analysis of surface enhancement by a porous substrate. *ASME Journal of Heat Transfer*, **112**: 700–706, 1990.

[21] V.R. Voller, C. Prakash. A fixed grid numerical modeling methodology for convection–diffusion mushy region phase-change problems. *Int. J. Heat Mass Transfer*, **30**: 1709–1719, 1987.

[22] H. Yoo, R. Viskanta. Effect of anisotropic permeability on the transport process during solidification of a binary mixture. *Int. J. Heat Mass Transfer*, **35**: 2335–2346, 1992.